

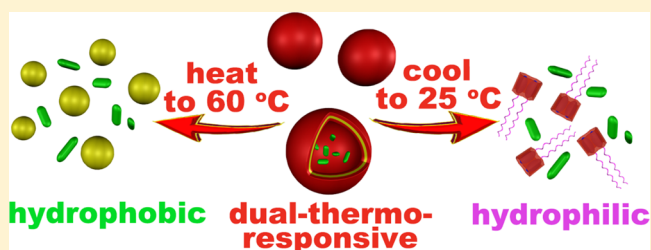
# A Dual-Thermoresponsive Gemini-Type Supra-amphiphilic Macromolecular [3]Pseudorotaxane Based on Pillar[10]arene/Paraquat Cooperative Complexation

Xiaodong Chi, Guocan Yu, Li Shao, Jianzhuang Chen, and Feihe Huang\*

State Key Laboratory of Chemical Engineering, Center for Chemistry of High-Performance & Novel Materials, Department of Chemistry, Zhejiang University, Hangzhou 310027, PR China

**S** Supporting Information

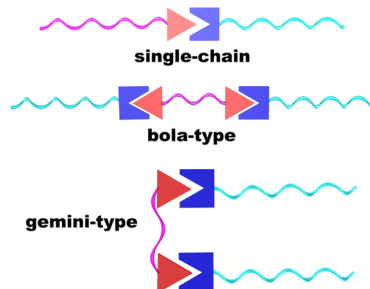
**ABSTRACT:** Herein, first we report the preparation of a thermoresponsive [3]pseudorotaxane from cooperative complexation between a water-soluble pillar[10]arene and a paraquat derivative in water. Then we successfully construct the first pillararene-based gemini-type supra-amphiphilic [3]pseudorotaxane from the water-soluble pillar[10]arene and a paraquat-containing poly(*N*-isopropylacrylamide) based on this new molecular recognition motif in water. This macromolecular [3]pseudorotaxane shows unique dual-thermoresponsiveness. Furthermore, it can self-assemble into polymeric vesicles at 37 °C in water. These vesicles can be further used in the controlled release of small molecules induced by cooling to 25 °C or heating to 60 °C.



## INTRODUCTION

For supra-amphiphiles, hydrophilic and hydrophobic groups are connected by noncovalent interactions.<sup>1</sup> Compared with traditional covalent amphiphiles, supra-amphiphiles can be prepared through comparatively convenient and environmentally friendly strategies. Moreover, they can be exquisitely designed to get well-defined self-assembly nanostructures through intelligent design of the building blocks. Up to now, various kinds of supra-amphiphiles have been studied, such as single-chain,<sup>2</sup> bola-type<sup>3</sup> and gemini-type<sup>4</sup> supra-amphiphiles (Scheme 1). For a gemini-type supra-amphiphile, two hydro-

**Scheme 1. Various Kinds of Supra-amphiphiles**



phobic tails and two hydrophilic headgroups are noncovalently linked by a spacer. Compared with single-chain and bola-type supra-amphiphiles, gemini-type supra-amphiphiles' hydrophobic chains stay closer to each other, permitting tighter molecular packing at the water–air interface.<sup>5</sup> Thus, gemini-type supra-amphiphiles usually display higher surface activities than single-chain and bola-type supra-amphiphiles. On the basis

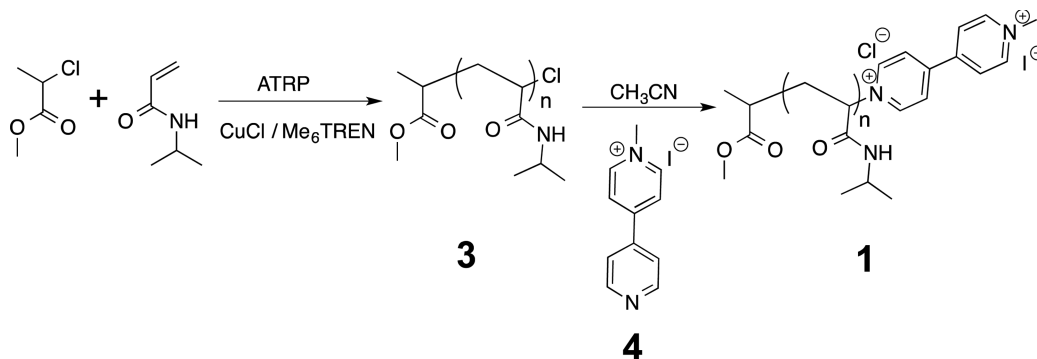
of this feature, they can be applied in many areas, such as nanodevices, sensor systems, cell imaging, and solubilization.<sup>4,6</sup> To date, the main method for preparing gemini-type supra-amphiphiles is the connection of oppositely charged single-tailed amphiphiles and “bola-type” organic salts together.<sup>7</sup> However, the existence of additional inorganic salts in the mixed “cationic” systems makes it difficult to study definite relationships between the structures of the gemini-type supra-amphiphiles and the well ordered assemblies. Besides, how noncovalent interactions affect the fabrication of gemini-type supra-amphiphiles is difficult to investigate. Therefore, it is essential to construct new kinds of gemini-type supra-amphiphiles through new methods, such as host–guest chemistry.

Pseudorotaxanes containing more than two components have been extensively explored not only because of their topological importance, but also due to their potential applications.<sup>8</sup> The inclusion of two guest molecules in a host has been reported.<sup>9</sup> For example, cucurbit[8]uril can bind two different types of guest molecules to form ternary complexes.<sup>9a,c</sup> However, it remains a challenging task for chemists to find new macrocycles to construct pseudorotaxanes by threading more than one guests through a macrocycle, since it is difficult to find a big enough host to encapsulate two or more guests in one ring efficiently.<sup>10</sup> Pillar[*n*]arenes,<sup>11</sup> a new class of supra-molecular hosts, can bind various kinds of guests to form pseudorotaxanes efficiently. They and pseudorotaxanes based on them have been actively applied in the construction of various interesting supramolecular systems, such as molecular

Received: December 16, 2015

Published: February 10, 2016

Scheme 2. Synthesis of Polymer 1



machines,<sup>12</sup> supramolecular polymers,<sup>11c</sup> amphiphiles and supra-amphiphiles,<sup>11h-j,l-o</sup> transmembrane channels,<sup>11k</sup> and nanostructures.<sup>11f</sup> Up to now, pillararene-based amphiphiles and supra-amphiphiles<sup>11h-j,l-o</sup> have been widely investigated. They have applications in many areas, such as drug/gene delivery, living cell imaging, and catalysis. However, pillararene-based gemini-type amphiphiles or supra-amphiphiles have never been reported; this restricts the further development of pillararene-based amphiphiles and supra-amphiphiles. Furthermore, pillararene-based thermoresponsive supramolecular systems have attracted great recent attention.<sup>13</sup> However, all of them have shown only a single thermoresponsive temperature. Here we present a unique dual-thermoresponsive gemini-type supra-amphiphilic [3]pseudorotaxane fabricated from water-soluble pillar[10]arene WP10 and paraquat-containing poly(*N*-isopropylacrylamide) (PNIPAM) 1 (Scheme 2) based on a novel and thermoresponsive 1:2 pillar[10]arene host/paraquat guest molecular recognition motif in water (Scheme 3). This [3]pseudorotaxane displays two thermoresponsive temperatures.

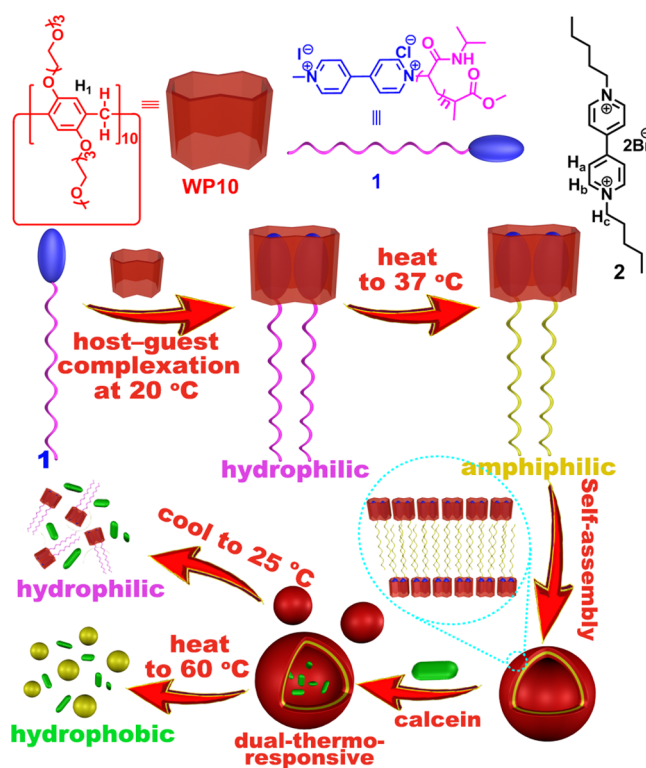
## EXPERIMENTAL SECTION

**Materials Preparation.** All reagents were commercially available and used as supplied without further purification. Compounds WP10<sup>13e</sup> and 2<sup>14</sup> were prepared according to published procedures.

**Synthesis of Polymer 3 (Scheme 2).** A mixture of isopropanol (25 mL) and hexamethyltris(2-aminoethyl) amine (Me<sub>6</sub>TREN, 0.75 mL, 1.0 equiv) was added to a 100 mL Schlenk flask containing *N*-isopropylacrylamide (NIPAM, 9.97 g, 30.0 equiv) and CuCl (0.291 g, 1.00 equiv), which was previously deoxygenated by degassing and backfilling with nitrogen twice. Then methyl 2-chloropropionate (0.32 mL, 1.0 equiv) was added to the solution. After stirring for about 10 min, the reaction mixture was stirred at 40 °C for 7 h. The polymerization was stopped through cooling by liquid nitrogen. The reaction mixture was dissolved in THF and stirred for additional 2 h, quickly passed through silica gel column, and precipitated into cold ethyl ether. The precipitate was collected by filtration and dried overnight in a vacuum to give polymer 3 as a white powder (5.77 g,  $M_{n,GPC} = 3.2$  kDa, PDI = 1.14). The <sup>1</sup>H NMR spectrum of compound 3 is shown in Figure S1. <sup>1</sup>H NMR (400 MHz, D<sub>2</sub>O, 298 K)  $\delta$  (ppm): 3.93 (broad, 27H), 3.72–3.69 (d, 3H), 2.44 (m, 1H), 2.2–2.0 (m, 27H), 1.81–1.20 (m, 54H), 1.16 (s, 162H).

**Synthesis of Polymer 1 (Scheme 2).** A mixture of polymer 3 (1.50 g, 0.480 mmol) and 4 (1.50 g, 5.00 mmol) in acetonitrile (50 mL) was stirred at 80 °C overnight. The solvent was evaporated and the residue was dissolved in 2 mL of THF. Then the solution was dropped into cold ethyl ether (100 mL, twice) and the precipitate was collected by filtration. The solid was dried overnight in a vacuum to give a light yellow powder. The <sup>1</sup>H NMR spectrum of polymer 1 is shown in Figure S3. <sup>1</sup>H NMR (400 MHz, CDCl<sub>3</sub>, 298 K)  $\delta$  (ppm): 8.94 (d,  $J = 4$  Hz, 2H), 8.80 (d,  $J = 4$  Hz, 2H), 8.42 (d,  $J = 4$  Hz, 2H),

Scheme 3. Chemical Structures of WP10, 2 and Polymer 1 and Schematic Illustration of Preparation of Polymeric Vesicles and Their Application in Dual-Thermoresponsive Release of Calcein Molecules



7.94 (d,  $J = 4$  Hz, 2H), 3.94 (broad, 27H), 3.74 (d,  $J = 8$  Hz, 3H), 3.57 (m, 5H), 2.17–2.01 (m, 27H), 1.82–1.41 (m, 52H), 1.16 (s, 162H).

**Transmission Electron Microscopy (TEM) and Dynamic Light Scattering (DLS) Studies.** TEM was used to reveal the aggregation structures of 1 and WP10 ⊃ 1<sub>2</sub>. A solution with a weight concentration of 2.00 mg/mL WP10 ⊃ 1<sub>2</sub> was prepared in water at 20 °C, and then gradually warmed to 37 °C (above the LCST of PNIPAM). The samples were prepared by drop-coating this solution on a carbon-coated copper grid. TEM experiments were carried out on a HITACHI HT-7700 instrument. Dynamic light scattering (DLS) measurements were carried out using a 200 mW polarized laser source Nd:YAG ( $\lambda = 532$  nm). The polarized scattered light was collected at 90° in a self-beating mode with a Hamamatsu R942/02 photomultiplier. The signals were sent to a Malvern 4700 submicrometer particle analyzer system.

**Critical Aggregation Concentration (CAC) Determination of WP10 ⊃ 1<sub>2</sub>.** Around the critical aggregation concentration, some parameters such as the conductivity, osmotic pressure, fluorescence intensity and surface tension of the solution change sharply. According

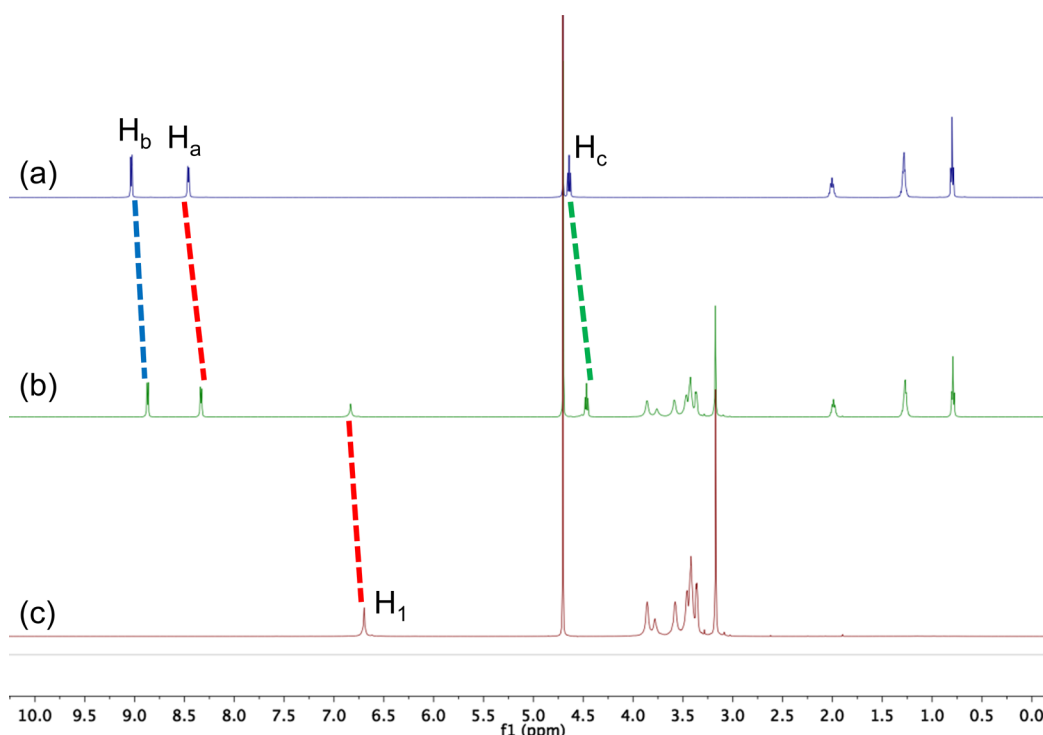


**Figure 1.** Partial  $^1\text{H}$  NMR spectra (400 MHz,  $\text{D}_2\text{O}$ ,  $25\text{ }^\circ\text{C}$ ): (a) 2.00 mM **2**; (b) 2.00 mM **WP10** with 2.0 equiv of **2**; (c) 2.00 mM **WP10**.

to this, the CAC determination of  $\text{WP10} \supset \mathbf{1}_2$  was performed by plotting the fluorescence intensity change versus the concentration using pyrene as a probe.

**Small Molecules (Doxorubicin and Calcein) Loading and Release of  $\text{WP10} \supset \mathbf{1}_2$  Vesicles.** Before loading doxorubicin (DOX) into vesicles, Doxorubicin hydrochloride was neutralized to DOX with excess amount of triethylamine before loading into the hydrophobic walls of the vesicles. A certain amount of DOX (in THF solution) was added to a solution containing **WP10** and **1**, then gradually warmed to  $37\text{ }^\circ\text{C}$ . After standing overnight, the prepared DOX-loaded vesicles were purified by dialysis in distilled water at  $37\text{ }^\circ\text{C}$  for several times. Calcein-loaded vesicles were prepared and dialyzed against deionized water until the water outside the dialysis tube showed insignificant calcein fluorescence.

The controlled release of the supramolecular vesicles in deionized water was performed as follows: 2 mL of a drug-loaded supramolecular vesicles solution was injected into a dialysis bag at  $37\text{ }^\circ\text{C}$ , and dialyzed against the deionized water solution at three different conditions ( $25$ ,  $37$ , and  $60\text{ }^\circ\text{C}$  for 24 h) for drug releasing. At certain time intervals, a 4 mL deionized water medium was removed and replaced by 4 mL of fresh deionized water.

## RESULTS AND DISCUSSION

**Host–Guest Complexation Studies.** First, the host–guest complexation between **WP10** and model guest **2** (Scheme 3) was investigated by  $^1\text{H}$  NMR spectroscopy (Figure 1). When 0.5 equiv of **WP10** was added to a solution of **2**, the resonance peaks corresponding to protons  $\text{H}_a$ ,  $\text{H}_b$ , and  $\text{H}_c$  on **2** shifted upfield by 0.16, 0.18, and 0.10 ppm, respectively. Additionally, the peaks of protons on **WP10** also exhibited chemical shift changes in the presence of **2** due to the host–guest interaction between **WP10** and **2**. All these chemical shift changes suggested that the complexation between **WP10** and **2** occurred in aqueous solution. Then, we carried out a 2D NOESY NMR experiment to investigate the relative positions of the components in the host–guest inclusion complex (Figure S6). Strong nuclear Overhauser effect (NOE)

correlations were observed between the signals corresponding to protons  $\text{H}_a$  and  $\text{H}_b$  on guest **2** and proton  $\text{H}_1$  of **WP10**, indicating that **2** was deeply embedded in the cavity of the pillararene moiety, in accordance with the results obtained from  $^1\text{H}$  NMR studies.

A mole ratio plot on the basis of the  $^1\text{H}$  NMR titration experiments proved that the complex between **WP10** and **2** had a 1:2 stoichiometry (Figure 2a). This was further confirmed by

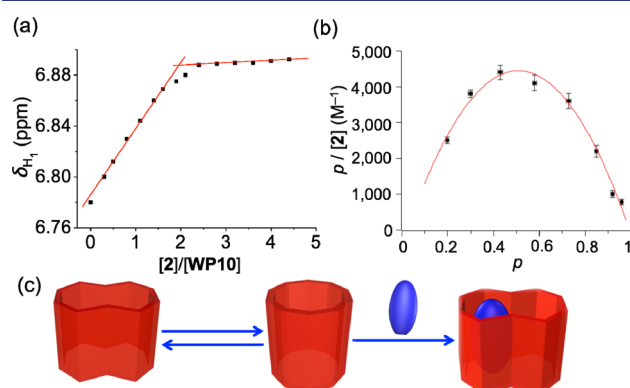


**Figure 2.** (a) Mole ratio plot for **WP10** and **2**, indicating the formation of a 1:2 host–guest complex. (b) Scatchard plot for the complexation of host **WP10** with guest **2** in  $\text{D}_2\text{O}$  at  $25\text{ }^\circ\text{C}$ .  $p$  = fraction of **WP10** units bound. Error bars in  $p$ :  $\pm 0.03$  absolute; error bars in  $p/[2]$ :  $\pm 0.06$  relative. (c) Cartoon representation of guest induced pillar[10]arene conformation change.

low-resolution electrospray ionization mass spectroscopy. As shown in Figure S5, peaks corresponding to  $[\text{WP10} \supset \mathbf{2}_2 - 4\text{Br}]^{4+}$  and  $[\text{WP10} \supset \mathbf{2}_2 - 3\text{Br}]^{3+}$  were monitored at  $m/z$  1185.21 and 1606.91, respectively.

In order to explore how the two binding sites of **WP10** affect each other during its complexation with paraquat derivative **2**,

we applied the Scatchard plot method<sup>15</sup> (Figure 2b), which is nonlinear and has a maximum, suggesting that the complexation between WP10 and 2 was cooperative. The association constants  $K_1$  and  $K_2$  for the complexation of WP10 with 2 were determined to be  $(8.3 \pm 0.1) \times 10^2 \text{ M}^{-1}$  and  $(6.2 \pm 0.3) \times 10^3 \text{ M}^{-1}$ , respectively (Figure S8). Actually, the ratio  $K_2/K_1 = 7.5$  is much higher than the value of 0.25 expected for statistical complexation.<sup>15</sup> Previous studies reported that there are two conformations of the pillar[10]arene ring in solution (Figure 2c). One conformation has two hexagon-like cavities,<sup>16</sup> and the other has a decagon-like cavity.<sup>17</sup> We propose that when WP10 binds the first paraquat unit, the conformation of WP10 tends to be the former and this preorganizes the pillar[10]arene ring for the complexation of the second paraquat unit (Figure 2c), explaining the cooperative complexation.

**LCST Behaviors of WP10 and PNIPAM 1.** In the previous work, Xue and coworkers reported that the host–guest complexation had an effect on  $T_{\text{cloud}}$  of the host.<sup>13e</sup> In view of this, we studied whether the binding of guest 2 had a similar effect on  $T_{\text{cloud}}$  of WP10. As shown in Figure 3, as the

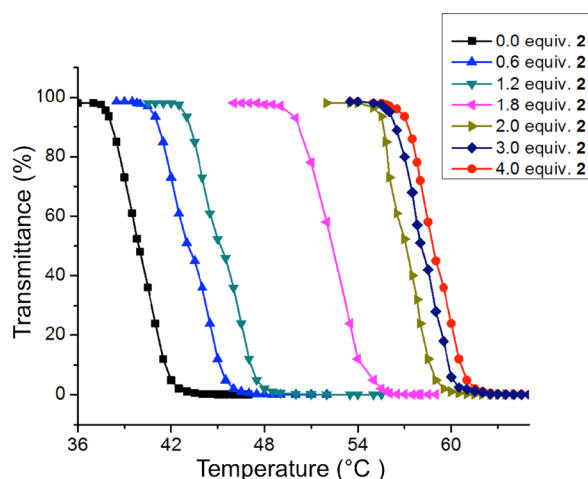


**Figure 3.** Temperature dependence of light transmittance of an aqueous solution of WP10 (2.00 mM) upon addition of 2 (0–8.00 mM) on heating. Heating rate: 2 °C/min.

concentration of 2 increased,  $T_{\text{cloud}}$  gradually increased while maintaining sharp transitions, indicating that  $T_{\text{cloud}}$  could be controlled by adding different amounts of 2 into the aqueous solution of WP10.

Then the effect of the added WP10 on the thermoresponsive behavior of PNIPAM 1 was explored by turbidity experiments. In the absence of WP10, PNIPAM 1 showed only a single-thermoresponsive profile (Figure 4, red solid line). However, by adding different amounts of WP10 to the aqueous solution of polymer 1, the curve of the turbidity changed dramatically. As shown in Figure 4, a dual-thermoresponsive profile gradually appeared as the concentration of WP10 increased, which arose from the formation of the gemini-type macromolecular supra-amphiphile.

**Thermoresponsive Host–Guest Complexation.** Then the thermoresponsiveness of the complexation between WP10 and 2 was investigated by <sup>1</sup>H NMR spectroscopy (Figure 5). Xue and co-workers recently found that WP10 showed LCST behavior.<sup>13e</sup> Hence, we supposed that the host–guest complexation between WP10 and 2 could be reversibly controlled by heating/cooling. As shown in Figure 5, when the temperature

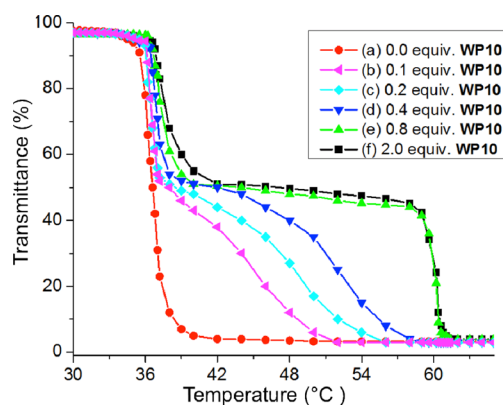


**Figure 4.** Transmittance changes of polymer 1 (2.0 mg/mL) with the addition of different amounts of WP10. Heating rate: 0.8 °C/min.

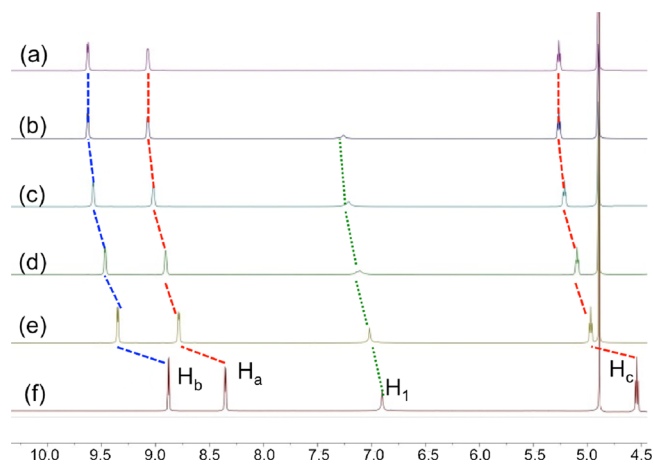


**Figure 5.** Partial variable temperature <sup>1</sup>H NMR spectra (600 MHz, D<sub>2</sub>O) of (a) 2 (2.00 mM) at 60 °C and 2 equiv of 2 and WP10 (2.00 mM): (b) 60 °C; (c) 55 °C; (d) 45 °C; (e) 35 °C; (f) 25 °C.

of an aqueous solution of WP10 and 2 was increased to 60 °C, the chemical shifts of the aromatic signals of the guest returned almost to their uncomplexed state (Figure 5, spectra a and b). However, the complex between WP10 and 2 reformed when the temperature of this solution was decreased to 25 °C. Thus, the complexation between WP10 and 2 can be reversibly controlled by heating and cooling.

**Microstructures of Self-Assembled Aggregates.** After establishment of the thermoresponsive complexation between WP10 and 2 in aqueous solution, we used paraquat functionalized polymer 1 and WP10 to construct a dual-thermoresponsive gemini-type supra-amphiphile (WP10 ⊃ I<sub>2</sub>) based on this molecular recognition motif. A solution with a weight concentration of 2.00 mg/mL WP10 ⊃ I<sub>2</sub> was prepared in water at 20 °C, and then gradually warmed to 37 °C (above the LCST of PNIPAM). UV–vis spectroscopy was measured to confirm the formation of the host–guest complex. As shown in Figure S9, when WP10 and 2 equiv of 2 were mixed together in water, the charge-transfer band of WP10 ⊃ I<sub>2</sub> appeared, indicating the formation of the inclusion complex.<sup>13a</sup> The critical aggregation concentration (CAC) of WP10 ⊃ I<sub>2</sub> was measured to be 0.12 mg/mL using pyrene as a probe molecule (Figure S10). To reveal the morphology of the self-assemblies formed from WP10 ⊃ I<sub>2</sub>, we carried out transmission electron microscopy (TEM) studies (Figure 6a), which showed spherical aggregates with an average diameter of ~160 nm.



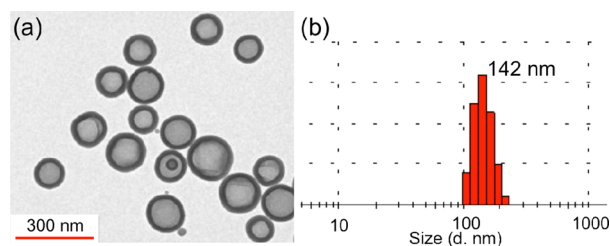


**Figure 6.** (a) TEM image of WP10 + 1 aggregates at 37 °C. (b) DLS data for WP10 + 1 aggregates at 37 °C.

From their darker thin wall and hollow cavity, we knew that the assemblies were polymeric vesicles. The wall thickness of the polymeric vesicles was measured to be about 18 nm based on TEM (Figure 6a). Moreover, DLS showed that the average size of the self-assemblies was about 142 nm (Figure 6b), close to the result from TEM.

On the basis of different LCST behaviors of the water-soluble pillar[10]arene WP10 and the poly(*N*-isopropylacrylamide) (PNIPAM) block of **1**, we succeeded in realizing dual-thermoresponsive self-assembly of the polymeric vesicles. First, we studied the transmittance changes of the self-assembled samples. As shown in Figure 4e, a transparent aqueous solution of WP10 ⊃ **1**<sub>2</sub> sharply turns opaque without precipitation when the temperature was increased from 20 to 37 °C, attributable to the solubility changes of the polymer chains. When the temperature was below the LCST of PNIPAM, the backbones of polymer were in random coil conformations and completely soluble in water due to the existence of hydrogen-bonds between the PNIPAM chains and water molecules. However, WP10 ⊃ **1**<sub>2</sub> changed from a water-soluble [3]pseudorotaxane into an amphiphilic gemini-type supra-amphiphile when the temperature was higher than the cloud-point temperature ( $T_{cp}$ ) of PNIPAM, because the hydrogen bonds were disrupted and the backbones of polymer collapsed into globular conformations and a soluble to insoluble phase change resulted. However, as the temperature was increased further, the sample precipitated; when the temperature reached the LCST of WP10, both polymer **1** and WP10 became hydrophobic, leading to the phase change and precipitation.

DLS was then used to monitor the thermoresponsiveness of supramolecular polymeric vesicles. When a solution of vesicles was cooled to 25 °C, the hydrophobic part of WP10 ⊃ **1**<sub>2</sub> became hydrophilic, and the average diameter of the assemblies sharply decreased from 142 to 6.8 nm (Figures 6b and 7a), indicating that no aggregation occurred at 25 °C. On the contrary, when the temperature of the aqueous solution was increased to 60 °C, the average size of the aggregates increased from 142 to 1484 nm (Figures 6b and 7b). This was attributed

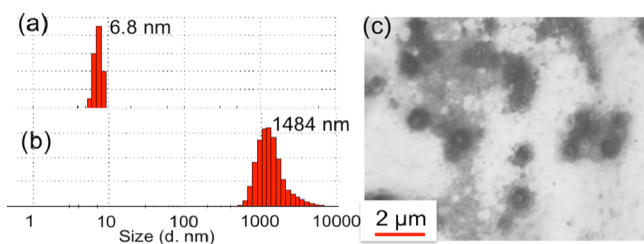


**Figure 7.** (a) DLS data of WP10 + 1 aggregates at 25 °C. (b) DLS data of WP10 + 1 aggregates at 60 °C. (c) TEM image of WP10 + 1 aggregates at 60 °C.

to the fact that the amphiphilicity of WP10 ⊃ **1**<sub>2</sub> was destroyed when the temperature exceeded the LCST of WP10. As a consequence, irregular precipitates were observed by TEM (Figure 7c). However, the average size of the assemblies returned to the original value by cooling the solution to 37 °C.

**Controlled Release.** The dual-thermoresponsiveness of the supra-amphiphilic [3]pseudorotaxane was then utilized in the controlled release of small molecules. Here hydrophilic calcein and hydrophobic DOX were used as model cargoes. In the absence of external stimuli, calcein only showed less than 25% release within 24 h. By cooling the solution to 25 °C or heating the solution to 60 °C, release of calcein molecules was achieved (Figures 8a and S12). Upon cooling the solution, a burst

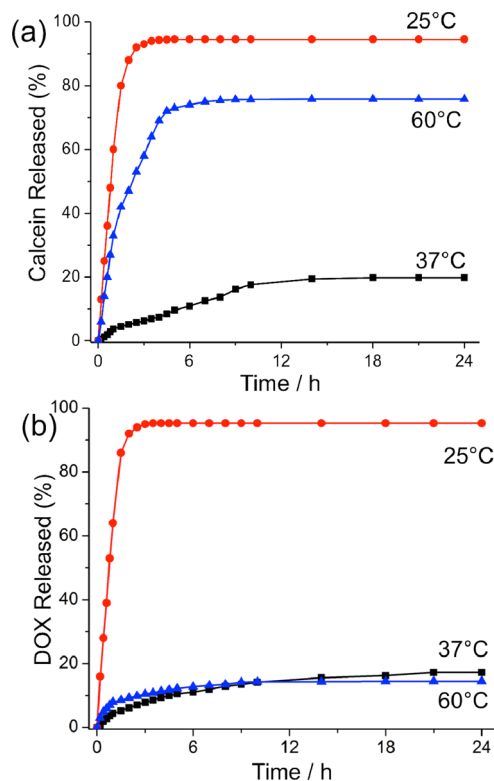


**Figure 8.** Controlled release of (a) hydrophilic calcein and (b) hydrophobic DOX from the polymeric vesicles as drug nanocapsules upon dual-thermo stimuli.

calcein release in the first 3 h was monitored and about 93% of the calcein molecules were released after 24 h. Upon heating the solution to 60 °C, only 60% of the calcein molecules were released over a period of 24 h. In the cooling process, the gemini-type WP10 ⊃ **1**<sub>2</sub> vesicles disassembled into water-soluble [3]pseudorotaxanes that are soluble in water, leading to the release of most encapsulated molecules. However, a portion of calcein molecules was encapsulated by the aggregates in the heating process. We then used these vesicles to encapsulate hydrophobic DOX since the walls of vesicles are hydrophobic. As shown in Figure 8b, a similar release trend was monitored when the temperature of the solution was at 25 °C. However, different release behavior was monitored at 60 °C. Because the aggregates changed from vesicles to solid aggregates, the released DOX was re-encapsulated, leading to a slow and less release of DOX (less than 20%). Thus, the supramolecular polymeric vesicles can serve as nanocapsules to load both

hydrophilic and hydrophobic cargoes that can be released by heating or cooling.

## CONCLUSION

In conclusion, we successfully established a new water-soluble thermoresponsive pillararene-based molecular recognition motif. It was found that WP10 formed a 1:2 [3]pseudorotaxane with paraquat derivative **2**. This complexation was cooperative as demonstrated by the Scatchard plot. Furthermore, based on WP10 and paraquat-containing homopolymer **1**, we utilized this molecular recognition motif to construct a pillararene-based macromolecular gemini-type supra-amphiphile, which self-assembled into vesicles in water above the LCST of polymer **1**. Because of the thermoresponsivenesses of WP10 and polymer **1**, as well as their different LCST behaviors, unique dual-thermoresponsiveness was achieved for this supra-amphiphile. The polymeric vesicles were further applied in the controlled release of water-soluble dye calcein and hydrophobic DOX. This work offers a new way to combine polymer science with pillararene supramolecular chemistry to construct functional supramolecular materials. Moreover, the new water-soluble pillar[10]arene-based 1:2 molecular recognition motif can be further employed in the construction of functional supramolecular systems with applications in various fields.

## ASSOCIATED CONTENT

### Supporting Information

The Supporting Information is available free of charge on the ACS Publications website at DOI: 10.1021/jacs.5b13173.

Experimental details and additional data. (PDF)

## AUTHOR INFORMATION

### Corresponding Author

\*fhuang@zju.edu.cn

### Notes

The authors declare no competing financial interest.

## ACKNOWLEDGMENTS

We thank the National Basic Research Program (2013CB834502), the NSFC/China (21434005, 91527301), the Fundamental Research Funds for the Central Universities, the Key Science Technology Innovation Team of Zhejiang Province (2013TD02), and Open Project of State Key Laboratory of Supramolecular Structure and Materials for financial support.

## REFERENCES

- (1) (a) Wang, C.; Wang, Z.; Zhang, X. *Acc. Chem. Res.* **2012**, *45*, 608–618. (b) Yu, G.; Jie, K.; Huang, F. *Chem. Rev.* **2015**, *115*, 7240–7303.
- (2) (a) Guo, D.-S.; Wang, K.; Wang, Y.-X.; Liu, Y. *J. Am. Chem. Soc.* **2012**, *134*, 10244–10250. (b) Wu, G.; Thomas, J.; Smet, M.; Wang, Z.; Zhang, X. *Chem. Sci.* **2014**, *5*, 3267–3274.
- (3) (a) Liu, Y.; Liu, K.; Wang, Z.; Zhang, X. *Chem. - Eur. J.* **2011**, *17*, 9930–9935. (b) Yao, Y.; Chi, X.; Zhou, Y.; Huang, F. *Chem. Sci.* **2014**, *5*, 2778–2782.
- (4) (a) Rodrigues, M.; Calpena, A. C.; Amabilina, D. B.; Ramos-López, D.; Lapuente, J. D.; Pérez-García, L. *RSC Adv.* **2014**, *4*, 9279–9287. (b) Wang, G.; Kang, Y.; Tang, B.; Zhang, X. *Langmuir* **2015**, *31*, 120–124.
- (5) Sorenson, G. P.; Coppage, K. L.; Mahanthappa, M. K. *J. Am. Chem. Soc.* **2011**, *133*, 14928–14931.

- (6) (a) Shimizu, T.; Masuda, M.; Minamikawa, H. *Chem. Rev.* **2005**, *105*, 1401–1444. (b) Yao, J.; Yang, M.; Duan, Y. *Chem. Rev.* **2014**, *114*, 6130–6178. (c) Zhang, G.; Hu, F.; Zhang, D. *Langmuir* **2015**, *31*, 4593–4604.

- (7) Shi, L.; Chen, F.; Sun, N.; Zheng, L. *Soft Matter* **2015**, *11*, 4075–4080.

- (8) (a) Huang, F.; Fronczek, F. R.; Gibson, H. W. *J. Am. Chem. Soc.* **2003**, *125*, 9272–9273. (b) Koshkakarayan, G.; Parimal, K.; He, J.; Zhang, X.; Abliz, Z.; Flood, A. H.; Liu, Y. *Chem. - Eur. J.* **2008**, *14*, 10211–10218. (c) Niu, Z.; Gibson, H. W. *Chem. Rev.* **2009**, *109*, 6024–6046. (d) Niu, Z.; Huang, F.; Gibson, H. W. *J. Am. Chem. Soc.* **2011**, *133*, 2836–2839. (e) Zhu, K.; Vukotic, V. N.; Loeb, S. J. *Angew. Chem., Int. Ed.* **2012**, *51*, 2168–2172. (f) Chen, L.; Tian, Y.; Ding, Y.; Tian, Y.; Wang, F. *Macromolecules* **2012**, *45*, 8412–8419. (g) Appel, E. A.; Loh, X. J.; Jones, S. T.; Biedermann, F.; Dreiss, C. A.; Scherman, O. A. *J. Am. Chem. Soc.* **2012**, *134*, 11767–11773. (h) Zhang, Q.; Qu, D.-H.; Wu, J.; Ma, X.; Wang, Q.; Tian, H. *Langmuir* **2013**, *29*, 5345–5350. (i) Li, S.; Huang, J.; Cook, T. R.; Pollock, J. B.; Kim, H.; Chi, K.-W.; Stang, P. J. *J. Am. Chem. Soc.* **2013**, *135*, 2084–2087. (j) Juríček, M.; Barnes, J. C.; Dale, E. J.; Liu, W.-G.; Struut, N. L.; Bruns, C. J.; Vermeulen, N. A.; Ghooray, K. C.; Sarjeant, A. A.; Stern, C. L.; Botros, Y. Y.; Goddard, W. A., III; Stoddart, J. F. *J. Am. Chem. Soc.* **2013**, *135*, 12736–12746. (k) Qi, Z.; Schalley, C. A. *Acc. Chem. Res.* **2014**, *47*, 2222–2233. (l) Isaacs, L. *Acc. Chem. Res.* **2014**, *47*, 2052–2062. (m) Ma, X.; Tian, H. *Acc. Chem. Res.* **2014**, *47*, 1971–1981. (n) Kim, S. K. K.; Sessler, J. L. *Acc. Chem. Res.* **2014**, *47*, 2525–2536. (o) Zhang, Z.; Cha, W.-Y.; Williams, N. J.; Rush, E. L.; Ishida, M.; Lynch, V. M.; Kim, D.; Sessler, J. L. *J. Am. Chem. Soc.* **2014**, *136*, 7591–7594. (p) Bruns, C. J.; Frascioni, M.; Iehl, J.; Hartlieb, K. J.; Schneebeli, S. T.; Cheng, C.; Stupp, S. I.; Stoddart, J. F. *J. Am. Chem. Soc.* **2014**, *136*, 4714–4723. (q) Wu, Y.-W.; Chen, P.-N.; Chang, C.-F.; Lai, C.-C.; Chiu, S.-H. *Org. Lett.* **2015**, *17*, 2158–2161. (r) Ma, X.; Zhao, Y. *Chem. Rev.* **2015**, *115*, 7794–7839.

- (9) (a) Kim, H.-J.; Heo, J.; Jeon, W. S.; Lee, E.; Kim, J.; Sakamoto, S.; Yamaguchi, K.; Kim, K. *Angew. Chem., Int. Ed.* **2001**, *40*, 1527–1529. (b) Liu, S.; Shukla, A. D.; Gadde, S.; Wagner, B. D.; Kaifer, A. E.; Isaacs, L. *Angew. Chem., Int. Ed.* **2008**, *47*, 2657–2660. (c) Appel, E. A.; Biedermann, F.; Rauwald, U.; Jones, S. T.; Zayed, J. M.; Scherman, O. A. *J. Am. Chem. Soc.* **2010**, *132*, 12351–14260.

- (10) (a) Huang, F.; Zakharov, L. N.; Rheingold, A. L.; Ashraf-Khorassani, M.; Gibson, H. W. *J. Org. Chem.* **2005**, *70*, 809–813. (b) Klotz, E. J. F.; Claridge, T. D. W.; Anderson, H. L. *J. Am. Chem. Soc.* **2006**, *128*, 15374–15375. (c) Prikhod'ko, A. I.; Sauvage, J.-P. *J. Am. Chem. Soc.* **2009**, *131*, 6794–6807.

- (11) (a) Ogoshi, T.; Kanai, S.; Fujinami, S.; Yamagishi, T.-a.; Nakamoto, Y. *J. Am. Chem. Soc.* **2008**, *130*, 5022–5023. (b) Cao, D.; Kou, Y.; Liang, J.; Chen, Z.; Wang, L.; Meier, H. *Angew. Chem., Int. Ed.* **2009**, *48*, 9721–9723. (c) Zhang, Z.; Luo, Y.; Chen, J.; Dong, S.; Yu, Y.; Ma, Z.; Huang, F. *Angew. Chem., Int. Ed.* **2011**, *50*, 1397–1401. (d) Strutt, N. L.; Forgan, R. S.; Spruell, J. M.; Botros, Y. Y.; Stoddart, J. F. *J. Am. Chem. Soc.* **2011**, *133*, 5668–5671. (e) Li, C.; Han, K.; Li, J.; Zhang, H.; Ma, J.; Shu, X.; Chen, Z.; Weng, L.; Jia, X. *Org. Lett.* **2012**, *14*, 42–45. (f) Li, H.; Chen, D.-X.; Sun, Y.-L.; Zheng, Y.; Tan, L.-L.; Weiss, P. S.; Yang, Y.-W. *J. Am. Chem. Soc.* **2013**, *135*, 1570–1576. (g) Fan, J.; Deng, H.; Li, J.; Jia, X.; Li, C. *Chem. Commun.* **2013**, *49*, 6343–6345. (h) Duan, Q.; Yu, C.; Yan, L.; Hu, X.; Xiao, T.; Lin, C.; Pan, Y.; Wang, L. *J. Am. Chem. Soc.* **2013**, *135*, 10542–10549. (i) Zhang, H.; Zhao, Y. *Chem. - Eur. J.* **2013**, *19*, 16862–16879. (j) Zhang, H.; Ma, X.; Nguyen, K. T.; Zhao, Y. *ACS Nano* **2013**, *7*, 7853–7863. (k) Si, W.; Li, Z.-T.; Hou, J.-L. *Angew. Chem., Int. Ed.* **2014**, *53*, 4578–4581. (l) Strutt, N. L.; Zhang, H.; Schneebeli, S. T.; Stoddart, J. F. *Acc. Chem. Res.* **2014**, *47*, 2631–2642. (m) Li, Z.-Y.; Zhang, Y.; Zhang, C.-W.; Chen, L.-J.; Wang, C.; Tan, H.; Yu, Y.; Li, X.; Yang, H.-B. *J. Am. Chem. Soc.* **2014**, *136*, 8577–8589. (n) Chang, Y.; Yang, K.; Wei, P.; Huang, S.; Pei, Y.; Zhao, W.; Pei, Z. *Angew. Chem., Int. Ed.* **2014**, *53*, 13126–13130. (o) Cao, Y.; Hu, X.-Y.; Li, Y.; Zou, X.; Xiong, S.; Lin, C.; Shen, Y.-Z.; Wang, L. *J. Am. Chem. Soc.* **2014**, *136*, 10762–10769.

(12) Zhang, Z.; Han, C.; Yu, G.; Huang, F. *Chem. Sci.* **2012**, *3*, 3026–3031.

(13) (a) Ogoshi, T.; Shiga, R.; Yamagishi, T.-a. *J. Am. Chem. Soc.* **2012**, *134*, 4577–4580. (b) Ogoshi, T.; Kita, K.; Yamagishi, T.-a. *J. Am. Chem. Soc.* **2012**, *134*, 20146–20150. (c) Ogoshi, T.; Aoki, T.; Shiga, R.; Iizuka, R.; Ueda, S.; Demachi, K.; Yamafuji, D.; Kayama, H.; Yamagishi, T.-a. *J. Am. Chem. Soc.* **2012**, *134*, 20322–20325. (d) Dong, S.; Zheng, B.; Yao, Y.; Han, C.; Yuan, J.; Antonietti, M.; Huang, F. *Adv. Mater.* **2013**, *25*, 6864–6867. (e) Chi, X.; Xue, M. *Chem. Commun.* **2014**, *50*, 13754–13756. (f) Ji, X.; Chen, J.; Chi, X.; Huang, F. *ACS Macro Lett.* **2014**, *3*, 110–113. (g) Chi, X.; Ji, X.; Xia, D.; Huang, F. *J. Am. Chem. Soc.* **2015**, *137*, 1440–1443.

(14) Nelissen, H. F. M.; Kercher, M.; De Cola, L.; Feiters, M. C.; Nolte, R. J. M. *Chem. - Eur. J.* **2002**, *8*, 5407–5414.

(15) Connors, K. A. *Binding Constants*; J. Wiley and Sons: New York, 1987; pp 78–86.

(16) Hu, X.-B.; Chen, Z.; Chen, L.; Zhang, L.; Hou, J.-L.; Li, Z.-T. *Chem. Commun.* **2012**, *48*, 10999–11001.

(17) Ogoshi, T.; Ueshima, N.; Sakakibara, F.; Yamagishi, T.-a.; Haino, T. *Org. Lett.* **2014**, *16*, 2896–2899.